IEEE Access
Multidisciplinary | Rapid Review | Open Access Journal

Received March 1, 2021, accepted March 14, 2021, date of publication March 19, 2021, date of current version March 26, 2021.

Digital Object Identifier 10.1109/ACCESS.2021.3067306

Effect of Build Orientation and Laser Power on Microwave Loss in Metal Additive Manufactured Components

RICHARD GUMBLETON[1], ROBERT BATSON[1], KENNETH NAI[2], AND ADRIAN PORCH[1]
[1]Centre for High Frequency Engineering, Cardiff University, CF24 3AA Cardiff, U.K.
[2]Group Engineering Division, Renishaw PLC, GL12 8JR Wotton-Under-Edge, U.K.

Corresponding author: Richard Gumbleton (gumbletonr1@cardiff.ac.uk)

This work was supported in part by the Engineering and Physical Sciences Research Council (EPSRC), and in part by Renishaw PLC through the Industrial Cooperative Awards in Science and Technology (ICASE) Studentship Program under Grant EP/R511882/1 and Grant EP/S513611/1.

ABSTRACT The adoption of metal additive manufacturing into the production of passive microwave components is still in its relative infancy. However, it is of increasing interest due to the offer of geometrical design freedom and significant weight reduction. The electrical properties of additive manufactured components are still inferior to traditional manufacturing techniques owing to the poor surface finish, especially on overhanging surfaces, which are unavoidable in three-dimensional microwave components. In this paper we present experimental findings on the disparity in microwave surface resistance values between three common build orientations, as well as findings that establish a connection between increasing downskin laser power and a reduction in surface resistance for overhanging surfaces. Finally, additive manufactured rectangular waveguide sections are measured to assess the influence of combined upward and downward facing surfaces on surface resistance.

INDEX TERMS Additive manufacture, metals, laser power, microwave, surface resistance, waveguide.

I. INTRODUCTION

Additive layer manufacturing (ALM) is of increasing interest within the aero/space industries due to its unique offering of unparalleled geometric design freedom. ALM produces parts with significant weight reduction compared with traditional manufacturing techniques, whilst maintaining up to 99.8% density [1]. Powder bed fusion (PBF), one form of ALM, uses spherical metal powder melted by a high power laser in successive layers to form three-dimensional components. A schematic of the PBF process is shown in Fig. 1. Although PBF adoption is still in relative infancy [2], many studies have been performed on their application to microwave communication components [3]–[5]. The electrical properties of PBF components are still inferior to machined alternatives [6], [7], however, the overall positive performance is somewhat surprising given the poor surface finish apparent on PBF surfaces. In particular, overhanging or downwards facing surfaces (with respect to the build direction) experience excessive dross formation and can generate significantly higher roughness than in other orientations [8], [9]. This suggests that some surfaces within a three-dimensional component will have better microwave performance than others, quantified in terms of microwave power loss. The main techniques used in literature to asses microwave PBF structures take a macro approach by measuring a complete waveguide component and comparing its performance to a traditional manufactured equivalent or simulation results [10], [11]. In this study, a more fundamental, experimental approach is taken; individual surfaces of different build orientations are assessed for microwave surface resistance (R_S), which are subsequently optimised through changes in PBF laser power.

The associate editor coordinating the review of this manuscript and approving it for publication was Xi Zhu.

II. BACKGROUND

A. MICROWAVE LOSS

At microwave frequencies, the skin effect causes electrical current to be carried in only the outermost regions of material at a depth known as the skin depth

$$\delta = \sqrt{\frac{1}{\pi f \mu \sigma}} \tag{1}$$

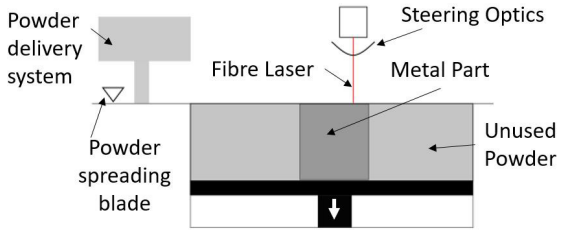

FIGURE 1. Schematic of the laser powder bed fusion manufacturing process. ©2019 Gumbleton *et al.* Reprinted from [12] (CC BY).

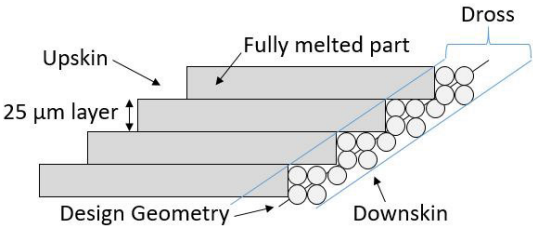

FIGURE 2. Schematic of dross formation on the downward facing surfaces during powder bed fusion manufacturing.

where f is the operating frequency (Hz), μ is magnetic permeability (H/m) and σ is electrical conductivity (S/m). For aluminium (of bulk conductivity $\sigma = 2.6 \times 10^7$ S/m) at a nominal frequency of 6.4 GHz (used in our characterisation experiments) the skin depth is calculated to be ≈ 1.2 μm. Therefore, with the majority of current carried at the surface of the material, even micro-surface features can have a significant impact on microwave loss; the relationship between roughness and microwave loss is well established in literature [13]. Power dissipation in a conductor at microwave frequencies is defined by

$$P_c = \frac{R_S}{2} \int_S |H_S|^2 dS \tag{2}$$

where S is the surface area on which the current flows (m^2), H_S is the tangential magnetic field at the metal surface (A/m) and R_S (Ω) is the quantifying metric for microwave loss, which encompasses surface roughness through an effective conductivity (σ_{eff}) as

$$R_S = \sqrt{\frac{\pi f \mu}{\sigma_{\text{eff}}}} \tag{3}$$

Since the average particle size is $\sim$47 μm for AlSi10Mg powder (with a range between 15 and 120 μm [14]) and $\delta \approx 1.4$ μm, it is justified to assume that the majority of current is flowing in one PBF layer. Therefore particular attention can be paid to optimising the outermost layers on each surface, such that the mechanical properties defined by the core PBF parameters remain unaltered. This is akin to the normal process of coating base metals such as brass with a thin layer of silver or gold for use in microwave components.

B. OVERHANG ROUGHNESS

The high degree of surface roughness seen on overhanging surfaces is, in part, attributed to dross formation, where a fraction of the laser energy penetrates below the desired layer and partially melts powder to the surface [15]; a representation of this phenomena is shown in Fig. 2. The adherence of partially melted powders is explained, at a fundamental level, by the surface energy of their spherical shapes. A sphere has the largest surface area for a shape of fixed volume, requiring less energy to form new bonds with other surfaces than is required to fully melt the powder [16].

In the context of PBF, 'downskin' is used to refer to a scan path which is not directly on top of a previously processed layer. The downskin applies to any downwards facing surface at an angle below the set activation angle, 60° in this case, relative to the build plate. Conversely, an 'upskin' refers to any laser path that does not have a proceeding layer directly above; each case has a different set of process parameters for manufacture. The downskin process parameters are set so that the laser raster passes several times over the dross region, melting more of the adhered powder with each pass. Studies have identified that for parts built in a 45° orientation, high laser energy density on the downskin layers can lead to a reduction in surface roughness [17], which may correlate to a reduction in surface resistance.

III. EXPERIMENTAL SETUP

Samples are prepared in AlSi10Mg using a Renishaw RenAM500 additive manufacturing system, which utilises a 500 W, ytterbium fibre laser of 1080 nm wavelength and 70 μm focal diameter. The samples have been built in horizontal, vertical and 45° orientations, as shown in Fig. 3, with varying laser power setups for vertical and 45° plates. The populated build plate is shown in Fig. 4. The default laser power for 45° upskin and downskin is 100 W, while the default laser power for the border scan on vertical built parts is 350 W, which are identified by (D) in Table. 1; these samples are used to quantify disparity in R_S between the different build orientations. The remaining samples are subjected to

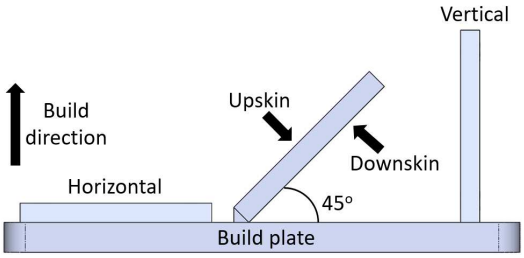

FIGURE 3. Schematic of the three build orientations used for sample manufacture.

TABLE 1. Laser power levels of 45° upskin and downskin and vertical built sample plates.

	45° Upskin & Downskin	Vertical
Power (W)	0, 60, 80, 100 (D), 120, 140, 160,	250, 270, 290, 310, 350 (D), 370, 410, 430, 450, 470,

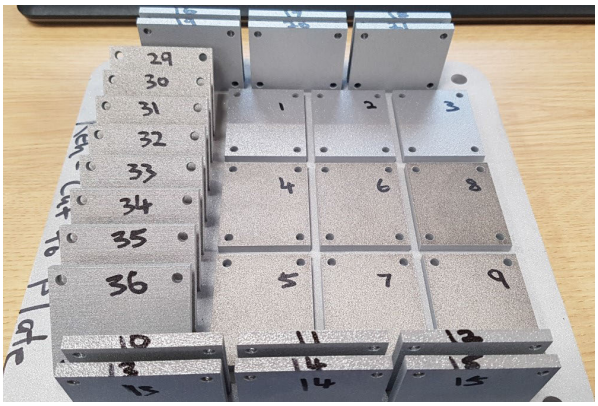

FIGURE 4. Photograph of the sample populated Renishaw RenAM500 additive manufacturing build plate.

variations in laser power levels, also shown in Table. 1, and are centered around the default values. All microwave characterisation measurements have been performed using a parallel plate resonator (PPR) setup, described in full in [18], where directional currents are induced in the study sample by the excitation of orthogonal resonant modes. The results reported here are measured at 6.4 GHz in the TEM_{010} resonant mode; a drawing of the PPR and simulations of its electric and magnetic fields, as well as induced current flow for this mode, are shown in Fig. 5. The reference plate is common to all measurements and its dimensions set the resonant frequency of the cavity, while the sample under test rests atop an indium gasket and is secured by bolts at each corner.

The operating principle of the PPR setup relies on the accurate measurement of quality (Q) factor while using a calibration sample before solving Eq. 4 to leave the sample R_{Ss} as the only unknown variable to be analysed when measuring a sample.

$$\frac{1}{Q_T} = G_s R_{Ss} + \sum_{m=1}^{i} G_{w_m} R_{Sw_m} + \sum_{p=1}^{j} p_{ed_p} \tan\delta_p \tag{4}$$

where Q_T is the total Q factor of the system, all measured Q factors are loaded values, including the effects of the coupling coefficients, and are corrected to produce unloaded values before calculation of surface resistance; the method is described in detail in [19]. R_{Ss} and G_s, R_{Sw} and G_w are the surface resistances and geometric values associated with the sample and the summation of i remaining conductive walls of the cavity, respectively, while p_{ed} is the dielectric filling fraction for j dielectric volumes present in the fixture. The geometric factors and dielectric filling fractions are defined as

$$G = \frac{1}{\omega} \frac{\iint_s \vec{H}_t \cdot \vec{H}_t^* ds}{\iiint_v \mu_0 \vec{H} \cdot \vec{H}^* dv} \tag{5a}$$

$$p_{ed} = \frac{\iiint_{vd} \varepsilon_d \vec{E} \cdot \vec{E}^* dv}{\iiint_v \varepsilon_v \vec{E} \cdot \vec{E}^* dv} \tag{5b}$$

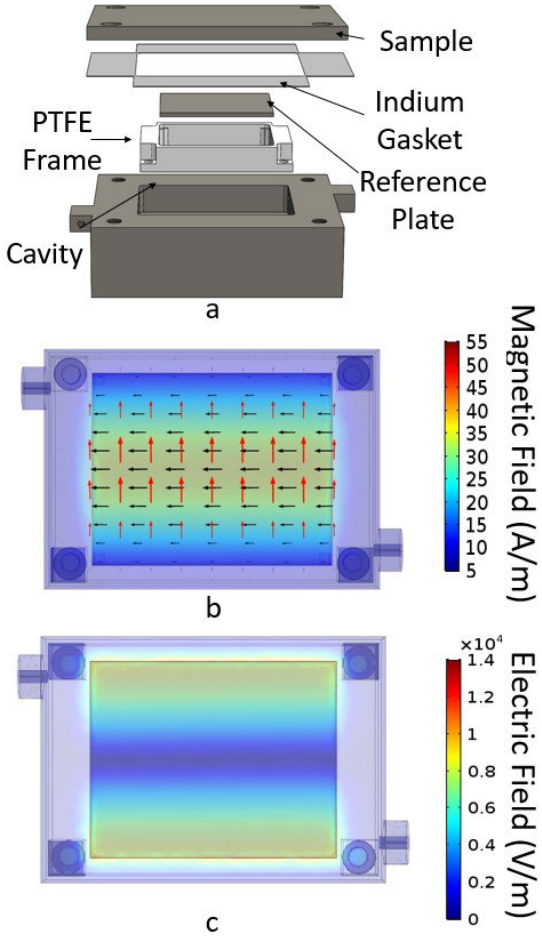

FIGURE 5. Parallel plate resonator fixture. a) Exploded CAD image and simulated electromagnetic properties for TEM_{010} mode at 6.4 GHz b) magnetic field (black arrows), magnetic field magnitude (color scale) and induced surface current (red arrows), c) electric field magnitude. Simulations are performed using COMSOL Multiphysics software with an arbitrary input power of 1 W. ©2021 IEEE. Reprinted, with permission, from IEEE [18].

where s is the surface integral for the conductive surface, v_d is the volume integral for the dielectric volume and v is the volume integral for the host cavity. μ_0 is the permeability of free space, and ε_d and ε_v are the permittivity of the component material and the material filling the cavity, respectfully. All microwave measurements were performed using a high precision Keysight N5232A vector network analyser.

IV. RESULTS AND DISCUSSION

A. BUILD ORIENTATION

Samples produced using default build parameters in different orientations have been measured for R_S and the results are shown in Fig. 6. The standard error reported on Fig. 6 is very small due to the high precision frequency measurement equipment used (Keysight N5232A network analyser), with less than 0.1% random error and the described cavity resonator fixture providing approximately 1% systematic error from the removal and replacement of samples. The 45° downskin surface, perhaps predictably, performs

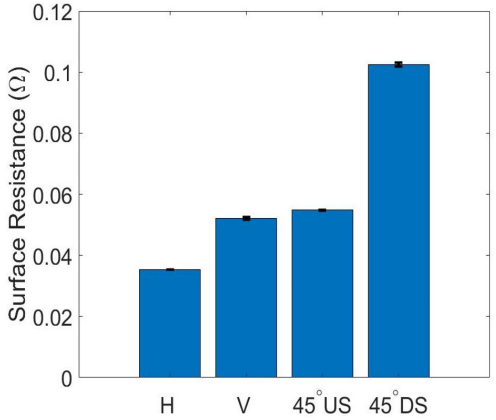

FIGURE 6. Measured surface resistance values for samples of different build orientation using default process parameters. Standard error is shown via error bars.

significantly worse in terms of microwave loss than other build orientations. Horizontal built plates exhibit the lowest loss of all samples, a result that supports previous measurements by this author [20], while there is only a marginal difference between vertical and 45° upskin surfaces. RMS surface roughness (R_q) measurements have been performed using a Taly Surf Series 2 drag profiler fitted with a tip of 2 μm radius and analysed with a 0.8mm cutoff low pass filter. R_q for the default values ($\sim$6 μm for horizontal, $\sim$12 μm for vertical, $\sim$13 μm for 45° upskin and $\sim$20 μm for 45° downskin orientations) correspond well with measured R_S, which increases with increasing surface roughness. From these results, it is evident that a macro approach to testing microwave components produced by PBF is missing important information regarding the specific locations where loss contributions are occurring and hence overall performance will be heavily dependent on the build orientation of the part.

B. LASER POWER

Fig. 7 shows the measured R_S values and R_q of 45° upskin and downskin surfaces and for samples built in a vertical orientation, against varying process laser power. In all cases R_S correlates well with observed changes in R_q. Fig. 7a and b correspond R_S values for vertical and 45° upskin surfaces, respectively; no significant pattern is observed relating R_S to changes in laser power. This may be explained for the upskin through the core build process having sufficiently melted the layer prior to the upskin parameters being implemented. Similarly, for the vertical built samples, border scans are repeated over successive layers, allowing for heat transfer through multiple layers such that a stable melt pool is generated, thus avoiding splutter and an excess of partially adhered powders.

Interestingly, the 45° downskin surfaces do exhibit a significant improvement with increasing laser power, shown in Fig. 7c. This is quantified by low values of R_S and correlates with lower values of R_q. Fig. 8 shows microscope images of the downskin surfaces for the worst (60 W) and best (180 W) performing samples. The 60 W sample (Fig. 8a)

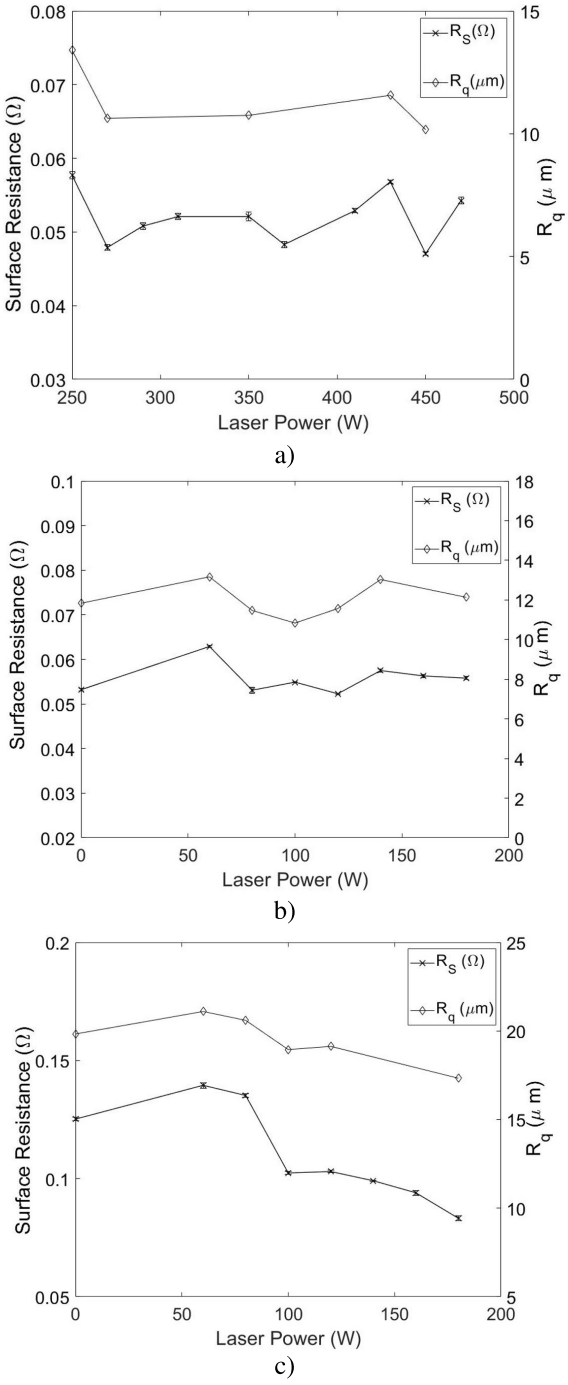

FIGURE 7. Graphs of measured surface resistance at different laser powers for a) vertical, b) 45° upskin and c) 45° downskin build orientations.

consists of an abundance of isolated satellites adhered only to the underlying surface. These partially melted powder spheres or satellites neither form a smooth surface or a sufficient electrical connection, and so are a major microwave loss contributor. In the 180 W sample (Fig. 8b), however, these satellites appears to have formed into larger agglomerates with surrounding particles, creating a more effective network of electrical connection and a more coherent layer. This is explained by the additional energy density penetrating deeper

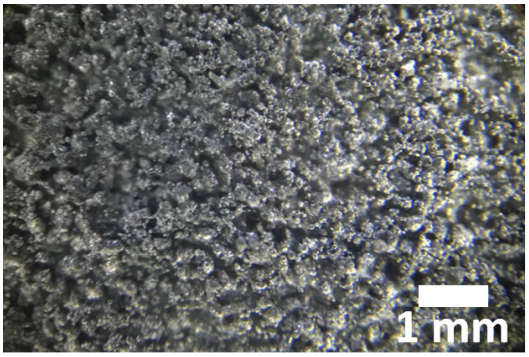

a)

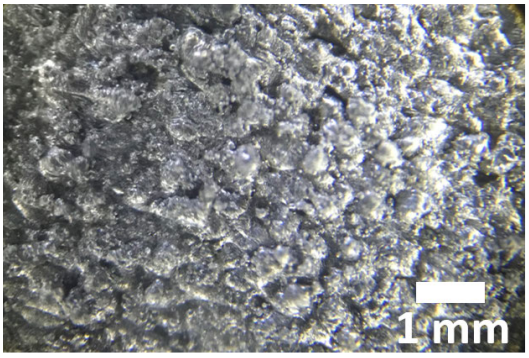

b)

FIGURE 8. Microscope images of 45° downskin surfaces manufactured with laser powers of a) 60 W and b) 180 W. Scale bar is set at 1 mm.

into this layer and more fully melting a greater proportion of the particles.

C. APPLICATION TO WAVEGUIDE COMPONENTS

To test the influence of the above laser power optimisation, a series of 45° orientated waveguide sections have been manufactured, as shown in Fig. 9a. The build orientations is such that two internal surfaces of each waveguide are upwards facing and use the default parameter setup, while the remaining downward facing surfaces are swept for each waveguide section using the following laser powers; ALM1 = 100 W (default), ALM2 = 0 W and ALM3 = 180 W. Fig. 9b shows one of these waveguide sections connected to a vector network analyser, through magnetic coupling loops, by using blank end flanges; this converts the waveguide transmission line section into a waveguide resonant cavity, allowing loss to be measured more reliably through Q factor than the attenuation from the measurement of transmitted power. Q factor and hence R_S are measured through the forward transmission S parameter S_{21}. These traces are shown as an inset to Fig. 10. The resonant frequency of the dominant TE_{101} mode of this air filled cavity is 6.62 GHz, a similar frequency to the PPR measurements for consistency of results and dictated by the internal geometry of the cavity; 22.86±0.06 mm × 10.16±0.1 mm × 154±0.1 mm. R_S for the cavity geometry is found by

$$R_{Sr} = \frac{1}{G\,Q_T} \tag{6}$$

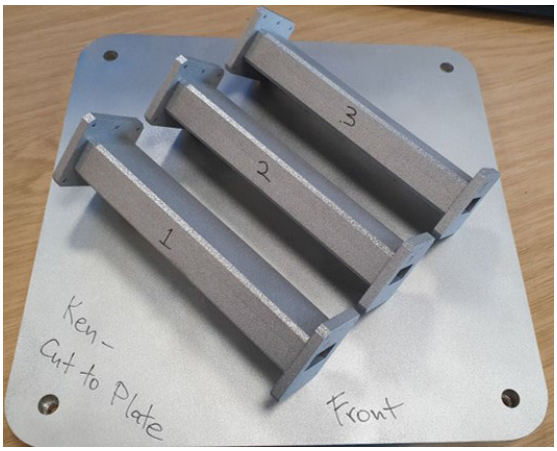

a)

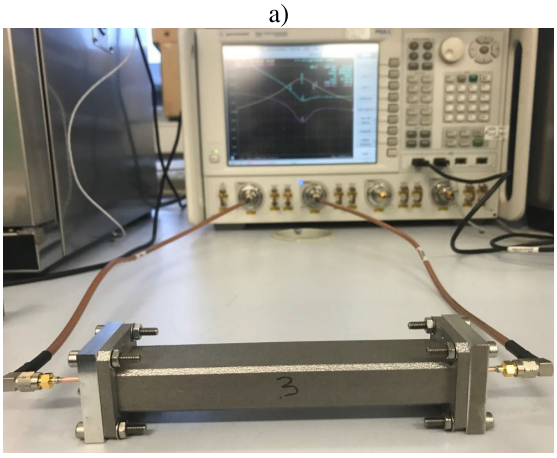

b)

FIGURE 9. Additive manufactured AlSi10Mg waveguide sections, a) post build and b) connected as a cavity resonator to a vector network analyser.

where G is found through simulation using COMSOL Multi-physics software. The measured R_S values for each waveguide section are shown in Fig. 10. There is a clear reduction in R_S for sample ALM3, arising from the use of 180 W for the downskin laser power, when compared to the default value (ALM1: 100 W) and the absence of a downskin layer (ALM2: 0 W). These results are promising for the optimisation of PBF produced parts for microwave applications.

To asses how the reduction in R_S will translate into a waveguide transmission line system, attenuation has been calculated using the measured resonator R_S (R_{Sr}) values over the X-band frequency range. Conductor attenuation (α_c) due to the surface conduction losses of a uniform, rectangular waveguide in the TE_{10} mode is assessed by [21]

$$\alpha_c = \frac{R_{Sr}(f)}{b\eta_0\sqrt{1-x^2}}\left[1+\frac{2bx^2}{a}\right] \tag{7}$$

where a and b are the long and short internal dimensions of the waveguide, respectively, and η_0 is wave impedance of free space. The dimensionless parameter x is defined as the ratio $x = f_c/f$, where $f_c = c/2a$ is the cut-off frequency of the TE_{10} mode and f is the frequency of single mode operation

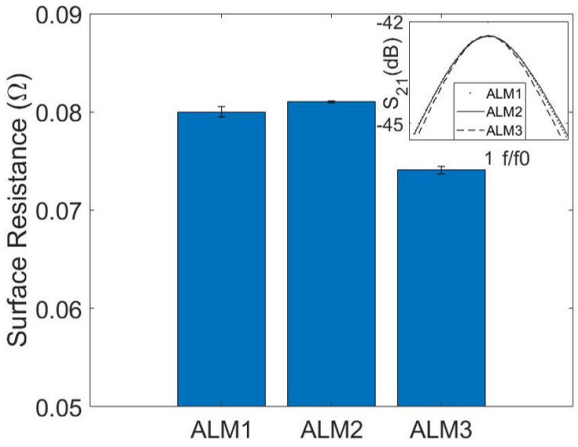

FIGURE 10. Measured surface resistance values for additive manufactured rectangular waveguide resonators produced using various down skin laser powers. Inset is the forward transmission S parameter traces for each waveguide resonator.

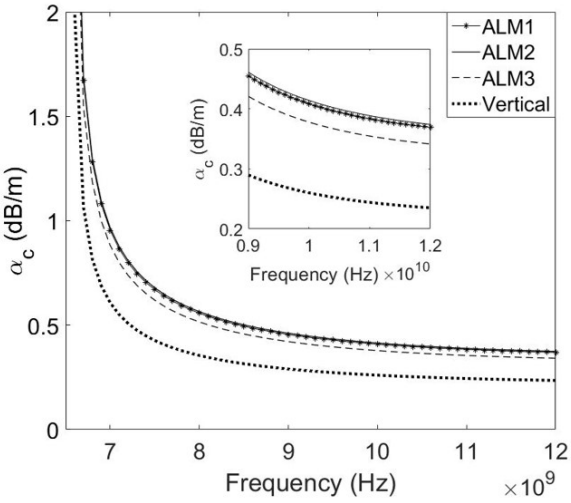

FIGURE 11. Calculated attenuation for TE_{10} mode of three rectangular waveguides produced by additive manufacturing using various downskin laser powers. Also included is a calculated value for an equivalent waveguide consisting of vertical surfaces. Inset is a magnified view of the calculated attenuation.

(i.e. in the range $c/2a < f < c/2b$). For calculation of α_c over the X-band frequency range, R_{Sr} is scaled from the cavity resonator measured value by

$$R_{Sr}(f) = R_{Sr}\sqrt{\frac{f}{for}} \tag{8}$$

Fig. 11 shows the calculated α_c values for each waveguide section over the X-band frequency range. The reduced R_S value for ALM3 provided a modest ∼0.05 dB/m improvement in conductor loss. For completeness, and to show the effect of build orientation on attenuation, a calculated value for an equivalent rectangular waveguide built in a vertical orientation is included on Fig. 11; the R_S value for this is taken from Fig. 6. Attenuation is significantly lower (∼0.13 dB/m) in the absence of downward facing surfaces.

V. CONCLUSION

In this study, additive manufactured sample plates orientated in three common build angles and several X-band waveguide sections have been manufactured from AlSi10Mg and evaluated for microwave loss. Sweeps of laser power on different parameter settings have been performed the following conclusions can been drawn:

1) The traditional macro approach to testing additive manufactured waveguide components has a significant flaw in that it does not take into account the notably higher loss contributions arising from downwards facing surfaces. Knowledge of the microwave surface resistance for each surface orientation should form part of the design-for-additive process.
2) A correlation has been established between increasing laser processing power and reduction of microwave surface resistance as well as average surface roughness for downwards facing surfaces.

Furthermore, this study has shown that it is possible to optimise additive manufactured components to improve microwave performance through the adaptation of build process parameters affecting the surface finish. However, the influence that increased laser power may be having on the mechanical properties of the surfaces has not been investigated here and would be a useful further study in the drive for increased industry uptake.

The results presented here are promising for the continued improvement in performance, and subsequent industrial uptake, of PBF components for microwave applications, where the design of three-dimensional parts will inevitably necessitate for one or more downward facing surfaces.

ACKNOWLEDGMENT

Information on the data underpinning the results presented here, including how to access them, can be found in the Cardiff University data catalogue at http://doi.org/10.17035/d.2021.0129673935.

Thanks is given to Prof. M Gumbleton at the School of Pharmacy, Cardiff University, for support with optical microscopy imaging.

REFERENCES

[1] N. T. Aboulkhair, N. M. Everitt, L. Ashcroft, and C. Tuck, "Reducing porosity in AlSi10Mg parts processed by selective laser melting," *Additive Manuf.*, vols. 1–4, pp. 77–86, Oct. 2014.

[2] H. Williams and E. Butler-Jones, "Additive manufacturing standards for space resource utilization," *Additive Manuf.*, vol. 28, pp. 676–681, Aug. 2019.

[3] S. H. Khajavi, J. Partanen, and J. Holmström, "Additive manufacturing in the spare parts supply chain," *Comput. Ind.*, vol. 65, no. 1, pp. 50–63, Jan. 2014.

[4] P. A. Booth and E. Valles Lluch, "Realising advanced waveguide bandpass filters using additive manufacturing," *IET Microw., Antennas Propag.*, vol. 11, no. 14, pp. 1943–1948, Nov. 2017.

[5] O. A. Peverini, M. Lumia, F. Calignano, G. Addamo, M. Lorusso, E. P. Ambrosio, D. Manfredi, and G. Virone, "Selective laser melting manufacturing of microwave waveguide devices," *Proc. IEEE*, vol. 105, no. 4, pp. 620–631, Apr. 2017.

[6] P. Booth and E. V. Lluch, "Enhancing the performance of waveguide filters using additive manufacturing," *Proc. IEEE*, vol. 105, no. 4, pp. 613–619, Apr. 2017.
[7] C. R. Garcia, R. C. Rumpf, H. H. Tsang, and J. H. Barton, "Effects of extreme surface roughness on 3D printed horn antenna," *Electron. Lett.*, vol. 49, no. 12, pp. 734–736, Jun. 2013.
[8] F. Calignano *et al.*, "High-performance microwave waveguide devices produced by laser powder bed fusion process," *Procedia CIRP*, vol. 79, pp. 85–88, Mar. 2019.
[9] A. Charles, A. Elkaseer, L. Thijs, V. Hagenmeyer, and S. Scholz, "Effect of process parameters on the generated surface roughness of down-facing surfaces in selective laser melting," *Appl. Sci.*, vol. 9, no. 6, p. 1256, Mar. 2019.
[10] B. Zhang and H. Zirath, "A metallic 3-D printed E-band radio front end," *IEEE Microw. Wireless Compon. Lett.*, vol. 26, no. 5, pp. 331–333, May 2016.
[11] M. D'Auria, W. J. Otter, J. Hazell, B. T. W. Gillatt, C. Long-Collins, N. M. Ridler, and S. Lucyszyn, "3-D printed metal-pipe rectangular waveguides," *IEEE Trans. Compon., Packag., Manuf. Technol.*, vol. 5, no. 9, pp. 1339–1349, Sep. 2015.
[12] R. Gumbleton, J. A. Cuenca, G. M. Klemencic, N. Jones, and A. Porch, "Evaluating the coefficient of thermal expansion of additive manufactured AlSi10Mg using microwave techniques," *Additive Manuf.*, vol. 30, Dec. 2019, Art. no. 100841.
[13] E. Hammerstad and O. Jensen, "Accurate models for microstrip computer-aided design," in *IEEE MTT-S Int. Microw. Symp. Dig.*, Washington, DC, USA, May 1980, pp. 407–409.
[14] V. J. Matjeke, C. Moopanar, A. S. Bolokang, and J. W. van der Merwe, "Effect of heat treatment time on the microstructure and mechanical deformation behavior of additive-manufactured AlSi10Mg components," *Prog. Additive Manuf.*, vol. 5, pp. 379–385, Jun. 2020.
[15] H. Chen, D. Gu, J. Xiong, and M. Xia, "Improving additive manufacturing processability of hard-to-process overhanging structure by selective laser melting," *J. Mater. Process. Technol.*, vol. 250, pp. 99–108, Dec. 2017.
[16] R. M. German, *Sintering Theory and Practice*. Hoboken, NJ, USA: Wiley, vol. 1996.
[17] J. C. Fox, S. P. Moylan, and B. M. Lane, "Preliminary study toward surface texture as a process signature in laser powder bed fusion additive manufacturing," in *Proc. Summer Top. Meeting: Dimensional Accuracy Surf. Finish Additive Manuf.*, 2016, pp. 168–173.
[18] R. Gumbleton, J. A. Cuenca, S. Hefford, K. Nai, and A. Porch, "Measurement technique for microwave surface resistance of additive manufactured metals," *IEEE Trans. Microw. Theory Techn.*, vol. 69, no. 1, pp. 189–197, Jan. 2021.
[19] D. Pozar, *Microwave Engineering*. Hoboken, NJ, USA: Wiley, 1998.
[20] R. Gumbleton, K. Nai, S. Hefford, and A. Porch, "Effects of post-processing treatments on the microwave performance of additively manufactured samples," in *Proc. 13th Eur. Conf. Antennas Propag. (EuCAP)*, Krakow, Poland, Mar./Apr. 2019, pp. 1–4.
[21] S. Ramo, J. R. Whinnery, and T. van Duzer, *Fields and Waves in Communication Electronics*, 3rd ed. Hoboken, NJ, USA: Wiley, 1994.

RICHARD GUMBLETON received the B.Eng. (Hons.) degree in electronic and communications engineering from Cardiff University, U.K., in 2017, where he is currently pursuing the Ph.D. degree in microwave engineering as part of an ICASE studentship award with Renishaw PLC.

His research interest includes additive manufacturing for microwave applications, specifically the characterisation and optimisation of additive manufactured surfaces.

ROBERT BATSON received the B.Eng. (Hons.) degree in electrical and electronic engineering from Cardiff University, U.K., in 2018, where he is currently pursuing the Ph.D. degree in microwave engineering as part of an ICASE studentship award with Renishaw PLC.

His current research interest includes measurement techniques that utilises microwave and millimeter wave structures to characterise and optimise additive manufacturing surfaces.

KENNETH NAI received the B.Sc. (Hons.) degree in electronics and electrical engineering and the Ph.D. degree in control systems from Loughborough University, U.K., in 1990 and 1995, respectively.

Since 1995, he has been with Renishaw PLC, Wotton-Under-Edge, U.K., where he is currently a Principal Engineer and he has developed products in the field of metrology systems, neuro-surgical robotics, and metal powder 3-D printers. He has been granted 12 U.S. patents. He is also a member of the Institution of Engineering and Technology and a Chartered Engineer.

ADRIAN PORCH received the M.A. degree in physics and the Ph.D. degree in low temperature physics from Cambridge University, Cambridge, U.K., in 1986 and 1990, respectively.

He is currently a Professor with the School of Engineering, Cardiff University, Cardiff, U.K., where he leads the Center for High Frequency Engineering. He has 34 years of experience in applying microwave methods to measure and understand the fundamental properties of electronic materials, with 165 relevant publications. More recently, he has developed microwave sensors and applicators across different disciplines, including new medical sensors and new methods in electron paramagnetic resonance spectroscopy.